JOURNAL OF APPLIED POLYMER SCIENCE VOL. 18, PP. 2887–2902 (1974)

An Experimental Study of the Relationship Between Rheological Properties and Spinnability in the Dry Spinning of Cellulose Acetate–Acetone Solutions

PHILLIP D. GRISWOLD and JOHN A. CUCULO, *Department of Textile Chemistry, North Carolina State University, Raleigh, North Carolina 27607*

Synopsis

The elastic and viscous properties of five cellulose acetate–acetone solutions, varying from 19.9% to 28.6% solids concentration, are independently determined at 60°C by capillary rheometry techniques. The viscous flow behavior of the solutions is determined over four decades of shear rate. The Bagley analysis is used to determine the entrance pressure drop and the true shear stress at various shear rates. A plot of the entrance pressure drop at the maximum experimental shear rate versus solution concentration undergoes a rapid increase in slope at 24.0% solids concentration, the significance of which is discussed with respect to the development of an elastically deformable chain entanglement network. The die swell behavior of the solutions at 60°C is determined on a commercial-type dry-spinning apparatus. When the die swell ratio is plotted versus volumetric flow rate, all five solutions are found to possess a characteristic curve with a distinct maximum. Photographs illustrating the variation of die swell with volumetric flow rate are shown. Die swell measurements are also shown to correlate well with entrance pressure drop measurements. The degree of spinnability of each cellulose acetate–acetone solution at 60°C is found by determining first godet speed at which one or more threads break abruptly. Spinnability is found to go through a maximum at 24.0% solids concentration. The rheological measurements and spinnability results are discussed through the aid of a single rheological parameter incorporating both elastic and viscous solution responses.

INTRODUCTION

Spinnability is perhaps the most fundamental problem in all fiber-spinning processes. Indeed, the ability of polymer melts and solutions to be extended into long, thin threads is the essential base of the synthetic fiber industry. Spinnability is of special importance in the dry-spinning process where emphasis is placed on spinning at near maximum jet stretch with a minimum occurrence of threadline breakage such that continuous, high-speed production is achieved. In dry spinning, spinnability is influenced by both solution rheological properties and heat and mass transfer rates. However, a rheological correlation approach should prove an instructive beginning, especially in light of the tremendous complexity involved in consideration of the heat and mass transfer phenomena.

In this study, five cellulose acetate–acetone solutions of varying concentration are rheologically characterized at 60°C with the Instron capillary

rheometer. In addition, the die swell behavior of the solutions is studied at 60°C to attempt to gain further insight into their elastic behavior. Then, the degree of spinnability of each solution is determined at 60°C on an industrial-type dry spinning apparatus. The objective of this work is to correlate solution elastic and viscous properties with spinnability in the dry-spinning process.

EXPERIMENTAL

Dry-Spinning Apparatus and Procedure

Dry-spinning experiments were conducted on an industrial-type dry-spinning system. Figure 1 illustrates the entire spinning system. It is composed basically of four sections: (1) solution preparation, (2) solution extrusion, (3) spinning cabinet, and (4) yarn take-up. A complete description is given elsewhere.[1] A 20-hole × 50-μ-diameter spinnerette, manufactured by Englehard Industries (Zurich, Switzerland), was used in this study. The spinnerette, which is constructed of type 316 stainless steel, has a 60° entrance angle and a length/diameter ratio of 1.0.

Each spinning solution was prepared in a Hamilton mixer with motor-driven stirring blades. Acetone and distilled water were first mixed so that the final ratio, including the water in the cellulose acetate, would be 94.2/5.8 on a weight basis. While the solvent was stirred, secondary cellulose acetate (CA) flakes were added. Cellulose acetate (Tennessee Eastman Co. E-394) with an intrinsic viscosity of 1.60 dl/gm in 99.4% acetone was used to prepare all the spinning solutions in this study. After mixing for 24 hr, the solution was transferred to the stainless steel storage tanks through the application of nitrogen pressure to the mixing kettle. The solution was then filtered for 72 hr by continuous circulation through the filter press. After the filtration step, the solution concentration was determined and a sample of the solution was collected for rheological characterization. Table I shows the concentrations of the five CA–acetone solutions used in this study.

Threadline force at the first godet was measured with a Rothschild tensiometer equipped with a 0–4 g head. The first godet speed was continuously monitored by a Moviport electronic speed indicator equipped with a photoelectric sensing head.

TABLE I
Concentrations of Cellulose Acetate–Acetone Solutions

Solution	% Solids
A	19.9
B	21.7
C	24.0
D	26.9
E	28.6

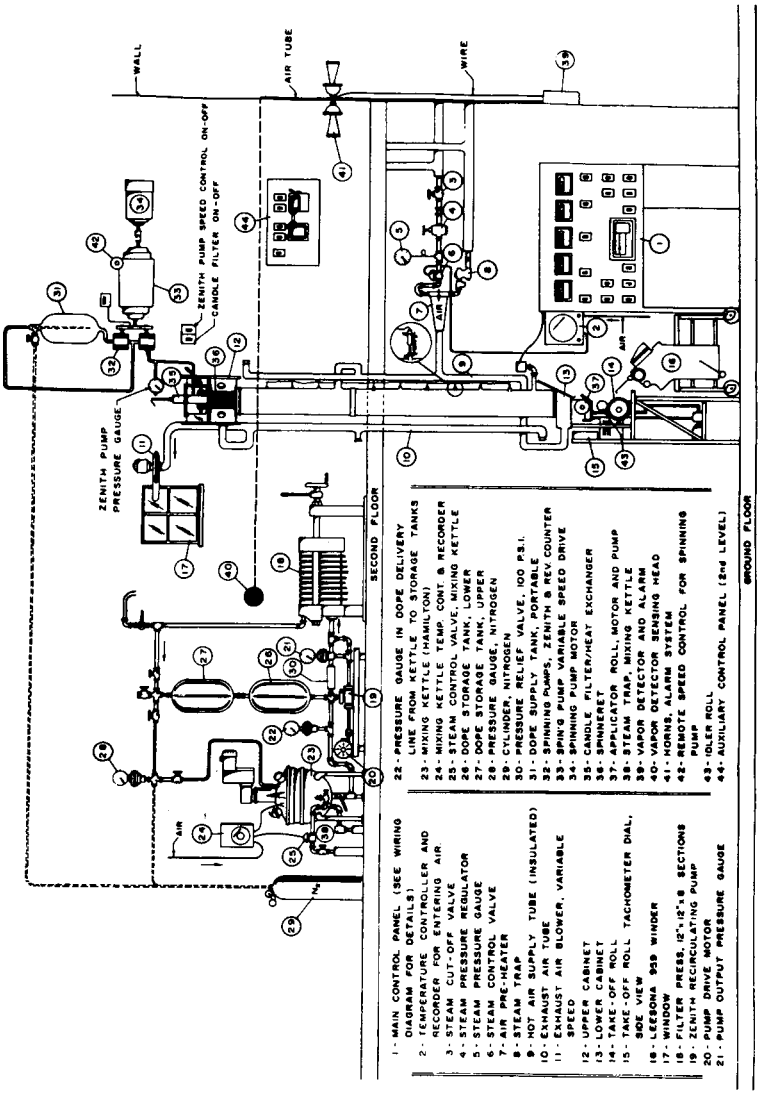

Fig. 1. Schematic of the experimental dry-spinning system.

The degree of spinnability of each of the five CA–acetone solutions was found by determining the maximum first godet speed $V_{1,m}$ of each solution at a constant jet velocity V.

All spinnability determinations were made with a spinning solution temperature of 60°C, and with top, center, and bottom spinning cabinet temperatures of 60°C, 70°C, and 80°C, respectively. During the spinnability runs, the exhaust air blower was not operated in order to allow accumulation of acetone vapor in the spinning cabinet and minimize formation of a filament "skin" in the elongational region of the threadline.

The starting point for all of the spinnability determinations was at a low first godet speed where spinning was obviously stable. Then the godet speed was slowly increased in 100 meters/min increments. At each increment, threadline stability was checked by allowing the system to operate for about 5 min. The rate at which the first godet speed was increased was about 25 meters/min/min, which could be regulated rather well owing to the continuous readout of godet speed by the speed indicator. During the course of the godet speed increases, a critical first godet speed $V_{1,m}$ was attained where one or more threads began to break near the spinnerette face. This critical speed was more precisely determined by decreasing the first godet speed slightly until spinning was stable and then slowly increasing the godet speed until breaks again occurred.

Rheological Characterization of Spinning Solutions

The rheological properties of the experimental spinning solutions were determined through the use of an Instron capillary rheometer. Table II lists the rheometer capillaries used in these rheological studies.

Capillaries A, B, and C were specially constructed for the measurement of entrance pressure drops. Capillary D was used to determine the flow curves and zero-shear rate viscosities of the CA-acetone solutions.

A simple loading apparatus was assembled which would quickly fill the rheometer reservoir with CA–acetone solution without the entry of air bubbles and loss of acetone. Loading was done at a barrel temperature of 52°C, 4° below the boiling point of acetone. Once loading was completed, the barrel temperature was quickly raised to 60°C, and the rheological characterization run was made.

TABLE II
Capillaries Used in the Rheological Studies of the Cellulose Acetate–Acetone Solutions

Capillary	Length L_c, in.	Diameter D_c, in.	L_c/D_c	Entrance angle, degrees
A	0.4695	0.0269	17.5	180
B	0.9459	0.0269	35.2	180
C	1.4190	0.0269	52.8	180
D	3.0000	0.03015	99.5	90

Values of entrance pressure drop ΔP_{ent} and true shear stress τ_{tw} were obtained by use of the well-known Bagley technique.[2] The Weissenberg-Mooney-Rabinowitsch analysis was applied to obtain true shear rate data for the viscous flow studies.

An apparatus consisting of a microscope tube mounted inside the working chamber of the spinning cabinet was used to measure and photograph the die swell of the CA–acetone solutions upon emergence from the extrusion section of the dry-spinning system. Photographs of die swell were made at selected levels of volumetric flow rate until a line gauge pressure of 500 psi was attained, beyond which distortion of the spinnerette was likely to occur.

RESULTS AND DISCUSSION

Solution Rheology

Determination of the viscous response to shear of the five CA–acetone solutions marked the first and most basic step in the rheological characterization phase of this work. Figure 2 shows the true flow curves of the solutions at 60°C. Note that in the range of concentrations considered, 19.9–28.6% solids, the solutions progress from mildly pseudoplastic to strongly pseudoplastic viscous flow behavior. Figure 3 shows a log-log plot of zero-shear rate viscosity η_0 versus solution concentration C for the solutions at 60°C. Note that a single straight line of slope 7.5 is obtained. Although there is yet no theory to completely explain a viscosity–concentration plot for polymer solutions, it is likely to be analogous to a Bueche plot of viscosity versus molecular weight for polymer melts.[3] Therefore, it appears that all the solutions used in this study possessed continuous entanglement networks of varying extent, since no inflection point is present in Figure 3. Hayahara and Takao[4] found log η_0–log C plots for concen-

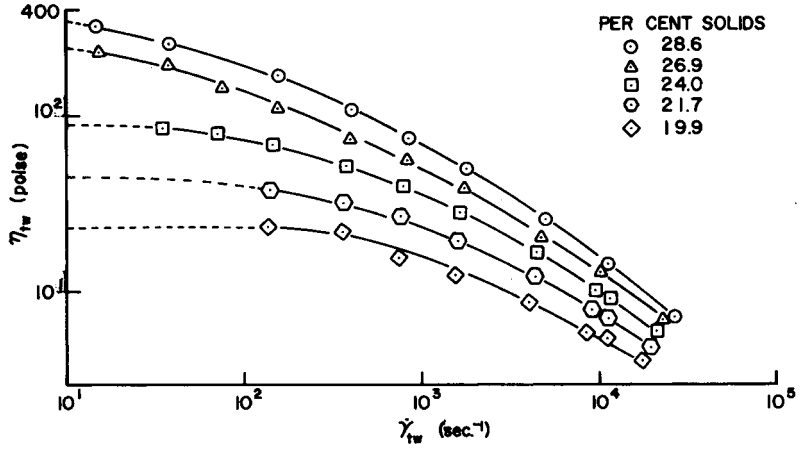

Fig. 2. True viscosity as a function of true shear rate for the cellulose acetate–acetone solutions at 60°C.

Fig. 3. Log zero-shear rate viscosity vs. log solution per cent solids for the cellulose acetate–acetone solutions at 60°C.

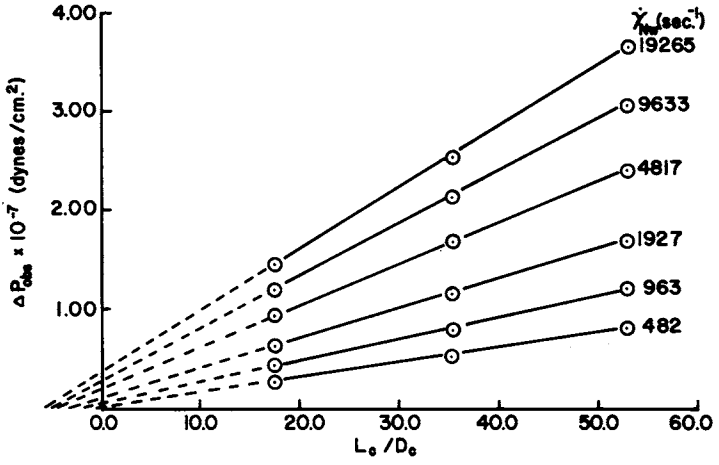

Fig. 4. Observed pressure drop vs. capillary length/diameter ratio at various shear rates for the 28.6% solids cellulose acetate–acetone solution at 60°C.

trated solutions of acrylonitrile copolymers to be linear with slopes of about 8. Since no inflection point was found in the concentration range of 25–60% solids, these authors assumed the existence of an inflection point at lower concentrations.

Figure 4 is a Bagley plot for the 28.6% solids CA–acetone solution at 60°C at various shear rates. A similar plot for the 19.9% solids solution showed that this solution does not develop a significant ΔP_{ent} value until the highest shear rate, 19265 sec^{-1}, is attained. Thus, it was decided that the ΔP_{ent} value at this maximum shear rate would be used to indicate the relative elasticity of the solutions.

Figure 5 shows a comparison of the Bagley plot at 19265 sec^{-1} for all five of the CA–acetone solutions at 60°C. Figure 6 utilizes data from Figure 5 to clearly show the variation of ΔP_{ent} and τ_{tw} with concentration. The

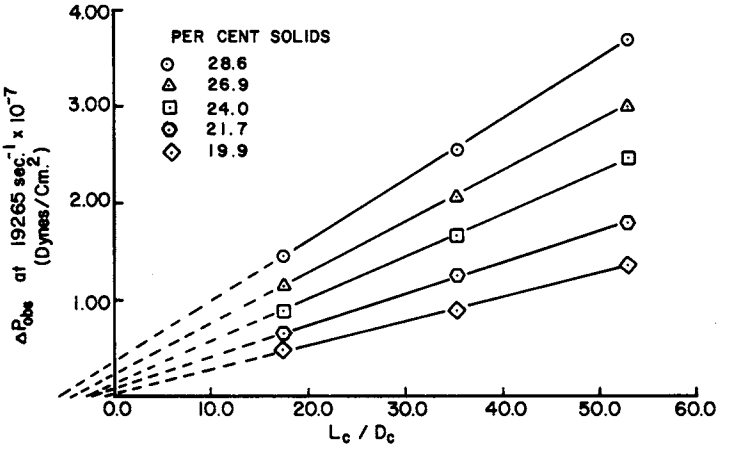

Fig. 5. Observed pressure drop at 19265 sec^{-1} vs. capillary length/diameter ratio for the cellulose acetate–acetone solutions at 60°C.

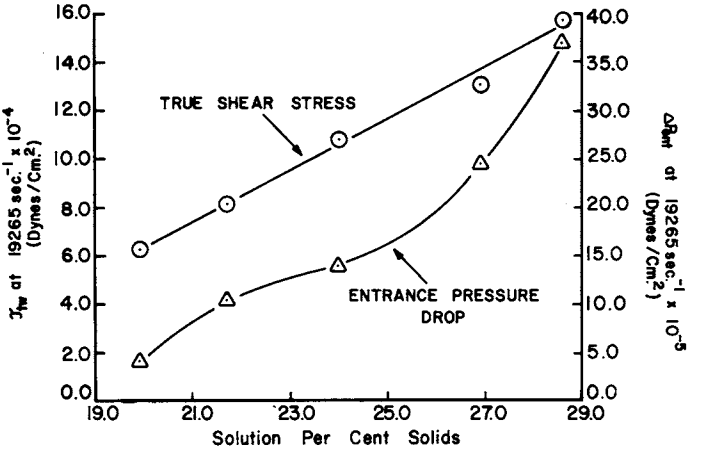

Fig. 6. True shear stress and entrance pressure drop at 19265 sec^{-1} as a function of solution concentration for the cellulose acetate–acetone solutions at 60°C.

variation of ΔP_{ent} at 19265 sec^{-1} with concentration permits some qualitative inferences to be made concerning the structure of the solutions studied. In recent years, investigators such as Schreiber et al.[5] and Hayahara and Takao[4] have advocated the existence of a critical molecular weight or solution concentration at which an elastically deformable entanglement network is formed. According to these authors, this elastic network should be formed at a higher critical molecular weight or concentration than would be found from a Bueche plot of viscosity versus molecular weight or concentration. Therefore, a much more extensive entanglement network would be required for the onset of elasticity than would be predicted by the segmental entanglement theory of Bueche.

The ΔP_{ent}–concentration plot in Figure 6 appears very intriguing since a rapid change of slope occurs at approximately 24.0% solids. It was previously concluded that all the CA–acetone solutions used in this study are sufficiently concentrated to permit either intramolecular or intermolecular segmental couplings. Yet it is likely that the ΔP_{ent}–concentration plot indicates that at about 24.0% solids, an entanglement network structure is formed which is sufficiently "long range" in nature to permit significant storage of elastic energy upon deformation. A "long range" entanglement network implies that a given polymer chain in the network is entangled with other chains at a sufficient number of points along its length so as to drastically restrict its random movement. Therefore, the long-range network is elastically deformable since it possesses a certain amount of structural integrity. The term "short range," then, might describe the entanglement structures of those CA–acetone solutions below 24.0% solids, where the lower entanglement frequency would allow viscous flow before significant elastic strain.

Die swell measurements were undertaken to provide greater insight into the elasticity of the five CA–acetone solutions. Measurements of the die swell ratio D_m/D_c, where D_m is the diameter of the fully recovered fluid stream under the existing conditions and D_c is the diameter of the extrusion capillary, were made using the extrusion section of the spinning apparatus.

In addition, the measurements were made utilizing a 20-hole × 50-μ-diameter spinnerette ($L_c/D_c = 1.0$) and at an extrusion temperature of 60°C, conditions identical to those used in the spinnability determinations. Die swell measurements of polymer solutions are usually made on a fluid extruded from a horizontal capillary to prevent draw-down effects. Although a vertical capillary was used in these experiments, gravitational effects were thought to be negligible since the polymer solutions were ejected from the capillary at very high velocities.

Just as a viscosity–shear rate plot may be used to characterize the viscous flow behavior of solutions, a die swell–volumetric flow rate plot may be used to characterize the elastic behavior. Figure 7 is such a plot for the five CA–acetone solutions at an extrusion temperature of 60°C. Curves similar to those in Figure 7 have also been observed by McIntosh[6] in his die swell experiments with 2% carboxymethylcellulose–water solutions. McIntosh utilized capillaries with L_c/D_c ratios of 50, 100, and 150 to ensure a well-developed velocity profile at the exit end of the tube. However, in the present experiments, it is interesting to note that a capillary with $L_c/D_c = 1.0$ was used.

The sequence of photographs in Figure 8 shows the variation of the shape and magnitude of the die swell with volumetric flow rate at 60°C. What appears as an upward-moving solution stream in the photographs is actually the reflection of the actual downward-moving solution stream on the face of the stainless-steel spinnerette. Thus, the capillary exit is at the plane of symmetry dividing the actual fluid stream and its reflection. Note in Figure 8 that D_m increases to a peak value at $Q = 21.5$ cm^3/min.

At higher values of Q, D_m decreases and approaches the diameter of the capillary.

Mention should be made concerning the possibile effect of heat and mass transfer on the magnitude and shape of the die swell phenomenon depicted

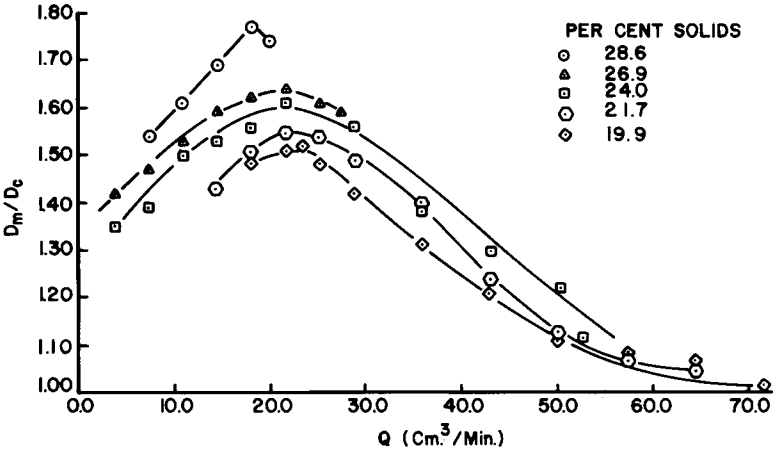

Fig. 7. Die swell ratio as a function of volumetric flow rate for the cellulose acetate–acetone solutions at 60°C.

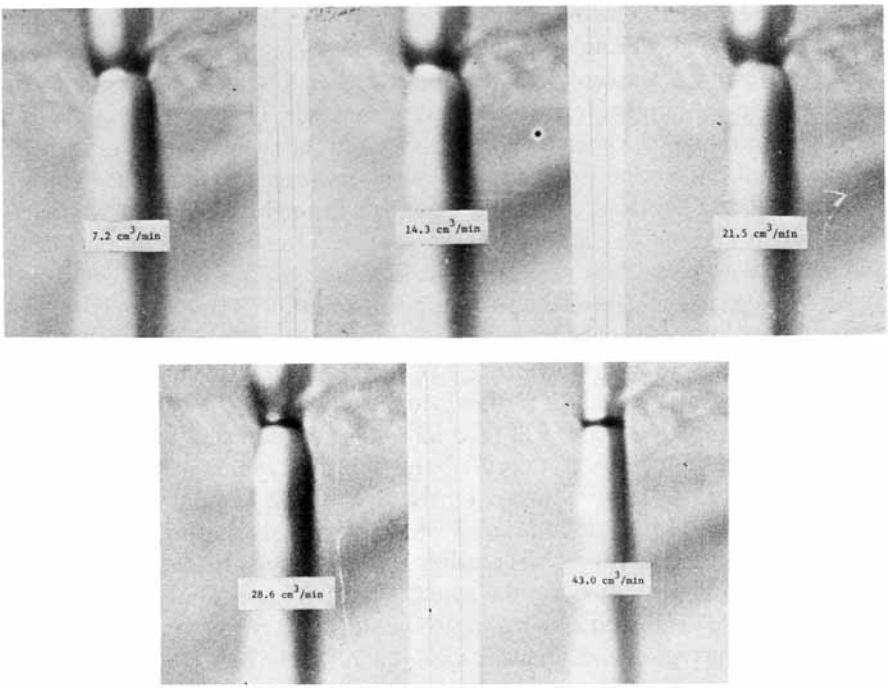

Fig. 8. Photographic sequence showing the variation of die swell with volumetric flow rate for a 24.0% solids cellulose acetate–acetone solution at 60°C. The solution is exiting a single capillary in a 20-hole × 50-μ-diameter spinnerette.

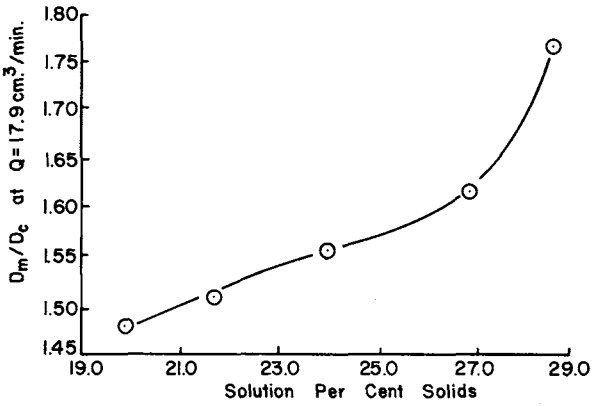

Fig. 9. Die swell ratio at a volumetric flow rate of 17.9 cm³/min vs. solution concentration for the cellulose acetate–acetone solution at 60°C.

in Figures 7 and 8. Two reasons may be given to explain why the evaporation of acetone may be considered to exert a negligible effect on the die swell of the CA–acetone solutions in this particular system. First, since the photographs of die swell involved such a small region near the spinnerette (on the order of 10^{-2} cm in length) and since the solutions were ejected at such high velocities, it is believed that significant loss of acetone was unlikely during the extremely short time span involved in the swelling process. Second, during these die swell measurements, the solutions were extruded into an ambient temperature atmosphere rather than the 60°C atmosphere used in the dry-spinning experiments. This factor should have further minimized the evaporation of acetone in the region of interest.

Although the mechanism for the die swell phenomenon shown in Figure 7 is undoubtedly complex, an initial explanation might consider a comparison of deformation time and material response. In the region of increasing die swell, it is very likely that the time of deformation t is large compared with the average response time τ of a given solution. Here, t may be approximated by the time of transit in the capillary. (Note that t decreases as Q increases). Thus, in the region of increasing die swell, there is sufficient time for a given solution to deform elastically in the capillary. The deformation of the solution will then increase with deformation rate, and a correspondingly greater recovery of the solution would occur when the elastic strain is allowed to decay at the exit of the capillary. However, as Q is increased, eventually a point will be attained where t will be small compared to τ, due to the decreasing transit time. In this case, there would be insufficient time for the solution to deform. Thus, the solution would undergo decreased strain and decreased strain recovery, which would account for the region of decreasing die swell in Figure 7.

Obviously, then, at the points of zero slope on the D_m/D_c–Q curves, one would expect that $t = \tau$. Note again in these curves that a shift in the curve peaks toward lower values of Q, and correspondingly higher values

of t, occurs as solution concentration increases. In the light of the previous explanation of this die swell phenomenon, one may conclude that this shift indicates that τ increases with solution concentration. This conclusion is certainly in agreement with well-known theory and experiment for the variation of material response times.

Figure 9 uses data from Figure 7 to show the variation of D_m/D_c at a reference Q value with solution concentration. A comparison of this curve with the ΔP_{ent}–concentration curve in Figure 6 reveals that both have strikingly similar shapes. Both possess an initial small increase in elasticity followed by a rapid increase at approximately 24.0% solids. Therefore, the existence of this increase in solution elasticity is supported by two distinct methods of investigation.

Threadline Breakage in the Dry Spinning of Cellulose Acetate–Acetone Solutions

Paul[7] and Han and Segal[8] utilized maximum first godet speed and maximum jet stretch as measures of spinnability in wet spinning. These parameters were also found to be useful in this study to determine spinnability in the dry-spinning process. Although the exact point of threadline failure could never be determined, breakage always occurred very close to the spinnerette face. Thus, it is reasonable to assume that breakage was confined to the elongational region of the spinning threadline, where the polymer solution stream is predominately fluid in nature. At low values of the first godet speed V_1, much lateral movement of the filaments in the elongational region was witnessed for all five CA–acetone spinning solutions due to the low imposed threadline tension. As V_1 was increased and was made to approach $V_{1,m}$, however, an interesting distinction was noticed in this lateral movement behavior of the low and high solution concentrations. For the two lowest solution concentrations, 19.9% and 21.7% solids, lateral movement of the threads continued as V_1 was increased and was even present to a great extent immediately before breakage at $V_{1,m}$. Immediately after the breakage, little recoil of the thread or threads was noticed. However, when the 24.0% solids solution was spun, the lateral movement behavior gradually diminished as V_1 was increased. For the highest solution concentrations, 26.9% and 28.6% solids, definite threadline response to V_1 was noted, with negligible lateral threadline movement present immediately before $V_{1,m}$. Considerable threadline recoil was noticed after breakage for the higher solution concentrations. Frequently, the recoil was of sufficient severity to cause adherence of spinning solution to the spinnerette face.

Figure 10 shows the variation of maximum first godet speed $V_{1,m}$ with volumetric flow rate Q for all five CA–acetone solutions at an extrusion temperature of 60°C. Through careful procedure, the reproducibility of $V_{1,m}$ values was good, particularly for the higher solution concentrations. Perhaps the most interesting feature of the linear plots in Figure 10 is the apparent slope difference which distinguishes the low and high solution

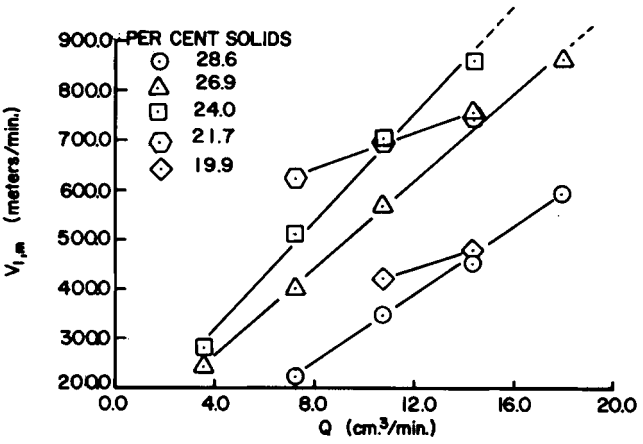

Fig. 10. Maximum first godet speed as a function of volumetric flow rate in the dry spinning of the cellulose acetate–acetone solutions at an extrusion temperature of 60°C.

concentrations. The $V_{1,m}$ values of the 19.9% and 21.7% solids solutions show a small dependence on Q when compared with the higher solution concentrations. This behavior may be made more understandable if one considers the rheological properties of the solutions. An increase in Q results in an increase in die swell for those values of Q considered in the spinning experiments. The force required to strain a material possessing an elastic network structure is directly proportional to the initial cross-sectional area. Thus, one may expect the most concentrated solutions, which possess well-developed chain entanglement network structures, to show a marked dependence on Q. The lower-per cent solids solutions, however, possess predominately viscous responses due to the short-range nature of their respective entanglement networks. Thus, $V_{1,m}$ may be expected to show a reduced dependence on Q for these solutions.

Figure 11 shows the variation of the maximum jet stretch $V_{1,m}/V$ at Q = 10.7 and 14.3 cm³/min, with solution concentration, using values of $V_{1,m}$ taken from Figure 10. Here, jet stretch is given by V_1/V, where V_1 is the first godet speed and V is the average velocity of the solution in the spinnerette capillary. The 24.0% solids solution appears to possess the highest degree of fiber spinnability of the five solutions studied, at both Q = 10.7 and 14.3 cm³/min. Since only five solutions were studied, the most spinnable solution concentration may not be determined precisely. Yet it is obvious that the 24.0% solids solution is not far from the true peak value.

Another interesting method of looking at spinnability is through the use of an apparent critical threadline tensile stress $(F/A)_c$, with solution concentration under the previously given dry-spinning conditions and a constant Q = 14.3 cm³/min. Figure 12 lends support to the previous conclu-

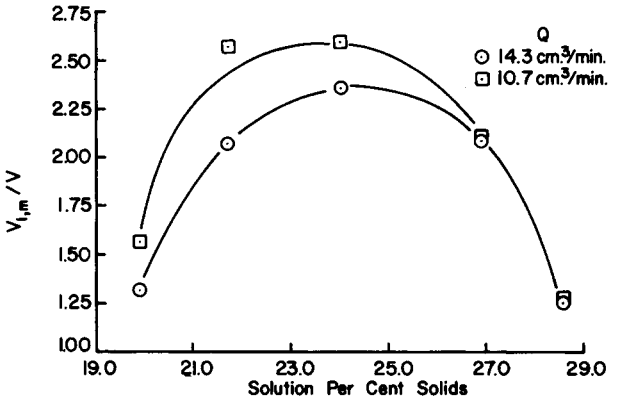

Fig. 11. Maximum jet stretch as a function of solution concentration in the dry spinning of cellulose acetate–acetone solutions at an extrusion temperature of 60°C.

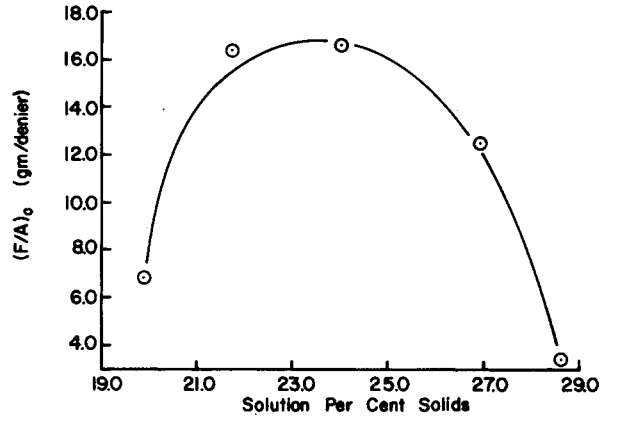

Fig. 12. Critical threadline tensile stress as a function of solution concentration in the dry spinning of cellulose acetate–acetone solutions at an extrusion temperature of 60°C. The volumetric flow rate is 14.3 cm³/min.

sion that the solution concentration of the highest degree of spinnability is very close to 24.0% solids. Yet the use of critical tensile stress also illustrates an important point concerning spinnability through the consideration of filament bundle denier. A spinning solution possessing a high degree of spinnability, as indicated by a high $(F/A)_c$ value, allows the high-speed production of a wide range of commercially important filament deniers with the desired mechanical properties. For example, continuous, high-speed production of low-denier filaments was achieved with the 24.0% solids solution. However, those solutions with low $(F/A)_c$ values proved to be severely restricted with respect to the production of commercially important filament deniers, since breakage occurred at high filament denier values.

Correlation Between Solution Rheological Properties and Spinnability

Figure 13 gives a comparison of rheological and spinnability parameters for the CA–acetone solutions used in this study. The upper plot shows the variation of the ratio $\Delta P_{ent}/\tau_{tw}$ at 19265 sec^{-1} versus solution concentration. Note that $\Delta P_{ent}/\tau_{tw}$ is a ratio of elastic to viscous stress and is a dimensionless number. The lower plot shows the variation of maximum free jet stretch $V_{1,m}/V_f$ versus solution concentration. V_f is defined as the velocity of the freely extruded solution stream, and is calculated from measured values of die swell. Free jet stretch was used by Han and Segal[8] as a more realistic measure of threadline attenuation in their wet spinning studies. By comparing these two plots, it may be readily seen that both a rheological and spinnability transition occurs at the solution concentration of 24.0% solids. It was hypothesized earlier that the rheological transition is a reflection of a change in the character of the solution entanglement network structure.

From that discussion, it is also reasonable to hypothesize that the transition point marks the change from solutions where viscous flow is the predominant rheological response to solutions where elastic strain is the predominant response. The maximum degree of spinnability must then be associated with an optimum combination of elastic and viscous solution components. Quantitatively, the optimum combination of solution rheological properties may be given by the $\Delta P_{ent}/\tau_{tw}$ parameter. In this study, the 24.0% solids solution gave a $\Delta P_{ent}/\tau_{tw}$ value of 13.1. It is

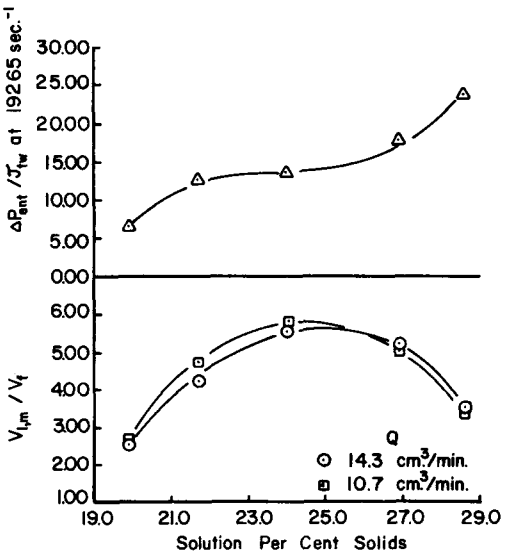

Fig. 13. Comparison of variation of the normalized entrance pressure drop and the spinnability criterion, maximum free jet stretch, with solution concentration for the cellulose acetate–acetone solutions at 60°C.

possible that $\Delta P_{ent}/\tau_{tw}$, or a similar dimensionless parameter where both viscous and elastic solution responses are considered, may be a critical value for solutions possessing maximum thread-forming ability. Such a parameter would be considerable improvement over the use of viscosity alone in the prediction of spinnability.

SUMMARY

The rheological properties of five cellulose acetate–acetone solutions were compared with their spinnability in the dry-spinning process.

The viscous behavior of the solutions in capillary flow at 60°C varied from mildly pseudoplastic to strongly pseudoplastic. Zero-shear rate viscosity η_0 was found to increase linearly with solution concentration in a log–log plot.

A rapid increase of the entrance pressure drop ΔP_{ent} at 19265 sec^{-1} occurred at 24.0% solids concentration. It was concluded that the rapid increase indicated the onset of a significant solution elasticity through the formation of a long-range entranglement network structure.

The die swell ratio D_m/D_c was found to initially increase, reach a peak value, and then decrease with volumetric flow rate Q for all solutions. The peak values were found to occur at lower values of Q as solution concentration increased.

The maximum attainable first godet speed $V_{1,m}$ appeared to be both a meaningful and reproducible measure of the degree of spinnability in dry spinning. The $V_{1,m}$ value was found to be a linear function of Q for all the solutions. Both the maximum jet stretch $V_{1,m}/V$ and the maximum free jet stretch $V_{1,m}/V_f$ showed that the 24.0% solids solution possessed the highest degree of spinnability of the solutions studied.

A comparison of rheological and spinnability data indicated that the 24.0% apparently possessed an optimum combination of elastic and viscous properties. It was proposed that a ratio of entrance pressure drop to true shear stress $\Delta P_{ent}/\tau_{tw}$, or another parameter similar to it, might aid in the prediction of spinnability.

The authors wish to thank Goodyear Tire and Rubber Company for their generous financial support. Gratitude is also extended to Beaunit Corporation, Research Triangle Park, North Carolina, for the use of the Instron rheometer and to Tennessee Eastman Company, Kingsport, Tennessee, for supplying the cellulose acetate flake.

References

1. R. W. Work and J. A. Cuculo, Technical Report AFML-TR-67-173 Pt. III, Submitted to Air Force Materials Laboratory, Air Force Systems Command, Wright-Patterson Air Force Base, Ohio, 1969.
2. E. B. Bagley, *Trans. Soc. Rheol.*, **5**, 355 (1961).
3. F. Bueche, *Physical Properties of Polymers*, Interscience, New York, 1962, p. 61.
4. T. Hayahara and S. Takao, *J. Appl. Polym. Sci.*, **11**, 735 (1965).

5. H. P. Schreiber, A. Rudin, and E. B. Bagley, *J. Appl. Polym. Sci.*, **9**, 887 (1965).
6. D. L. McIntosh, Ph.D. Thesis, Washington University, St. Louis, Missouri, 1960.
7. D. R. Paul, *J. Appl. Polym. Sci.*, **12**, 2273 (1968).
8. C. D. Han, and L. Segal, *J. Appl. Polym. Sci.*, **14**, 2999 (1970).

Received October 15, 1973
Revised March 25, 1974